

Wong, M.S., et al., 2023, Field calibration of $^{40}\text{Ar}/^{39}\text{Ar}$ K-feldspar multiple diffusion domain (MDD) thermal histories at the Grayback normal fault block, Arizona, USA: *Geology*, <https://doi.org/10.1130/G51319.1>

Supplemental Material

Sample collection and processing, $^{40}\text{Ar}/^{39}\text{Ar}$ analyses, modeling procedure, Tables S1–S8, and Figures S1–S10.

Field calibration of $^{40}\text{Ar}/^{39}\text{Ar}$ K–feldspar multiple diffusion domain (MDD) thermal histories at the Grayback normal fault block, Arizona

Martin S. Wong¹, Phillip B. Gans², and Damien Roessler¹

¹*Department of Earth and Environmental Geosciences, Colgate University, 13 Oak Drive, Hamilton, NY 13346*

²*Department of Earth Science, University of California, Santa Barbara, CA 93106*

Sample collection and processing

Samples were collected along a roughly east-west transect parallel to the slip direction within the block to sample a range of paleodepths. When possible, samples were collected near sample locations from prior work to facilitate comparison of the results. Efforts were taken in the field to avoid collection of samples that were altered or highly deformed. Samples were further screened for alteration in the lab through optical and scanning electron microscopy. Samples were crushed and sieved to 125-180 microns grain-size, floated in methylene iodide with a specific gravity = 2.59 and then hand-picked to a purity >99%. Splits of the final separate were analyzed using energy dispersive spectroscopy (EDS) on the scanning electron microscope to ensure a high level of purity.

$^{40}\text{Ar}/^{39}\text{Ar}$ analyses

$^{40}\text{Ar}/^{39}\text{Ar}$ analyses were conducted at both UC Santa Barbara and Lehigh University. J-values were calculated using Taylor Creek Rhyolite sanidine (UCSB) with an assumed age of 27.92 Ma (Duffield and Dalrymple, 1990) and biotite standard GA-1550 (Lehigh) as a neutron fluence monitor with an assumed age of 98.79 Ma (Renne et al., 1998). Samples were step heated in a double vacuum resistance furnace and temperatures were monitored with a thermocouple at the base of the crucible. Duplicate and often triplicate isothermal steps were conducted throughout the heating schedule to assess the degree of excess ^{40}Ar ($^{40}\text{Ar}_E$) present in the sample.

MDD modeling procedures

The domain structures for all samples were modeled using the *domains* program (P. Zeitler, *pers. comm.*), which runs the core routines and algorithm of the *autoarr* program (Lovera, 1992) with additional linear regression options and plot outputs. The *autoarr* program and other related software are available at this link:

<http://sims.ess.ucla.edu/argonlab/argon.htm>

Samples were modeled using an infinite slab geometry. Step heating experiments above 1100 °C were ignored for modeling purposes because this typically exceeds the melting temperature of K-feldspar *in vacuo*. The diffusion coefficients E (activation energy) and $\log(D_0/r_0)$ were calculated using the low-temperature linear portion of the Arrhenius plot (Lovera et al., 1997). A range of potential E values can be fit to the linear low temperature data and we typically used the best-fit

unweighted linear regression of these data for our modeling. However, we also explored a range of E values with reasonable fits to the data to understand how this value impacted the modelling results. It is important to note that the E value only impacts the absolute temperature values of the thermal model and not its fundamental form. When a range of E values were possible for a given sample, we also incorporated other constraints such as other thermochronologic constraints and geologic/structural controls to provide a best fit thermal history to all available constraints. Uncertainties in the E value on the linear regressions in this study ranged from ~1.3–5.9 kcal/mol and at the higher uncertainties, this translates into ca. ± 25 °C uncertainties in the absolute temperatures of the models, which are reflected in Figure 3. We constrained domain modeling to include 8–10 domains and modeled activation energy (E) ranged from 38.1–46.5 kcal/mol (mean = 43.1 kcal/mol). Samples GR-19 and GR-27, with E values of 40.5 and 38.1 kcal/mol respectively, have lower than the “typical” E value of 46 ± 6 kcal/mol reported by Lovera et al. (1997). Sample GR-19 is from the Proterozoic Ruin granite, which has a megacrystic texture and sample GR-27 is from a pegmatite dike within the ca. 70 Ma Tea Cup pluton, so these geologic differences may account for their lower E value. The remaining samples from the Cretaceous Tea Cup pluton (GR-1, GR-2 and GR-8) yield E values that range from 44.7–46.5 kcal/mol, which are more typical values.

We used the *Arvert 4.0* program (Harrison et al., 2005) to conduct inverse modeling to generate possible thermal histories given the diffusion domain structure and the measured age spectrum. The program uses a Monte Carlo approach to generate random thermal histories within a set of user-provided constraints. By necessity, portions of the modelled thermal history extend beyond the constraints provided by the $^{40}\text{Ar}/^{39}\text{Ar}$ K-feldspar data. These unconstrained portions of the thermal history are not shown in Fig. 3 but are shown in the data repository figures for completeness. The initial Monte Carlo set of thermal histories is used to generate synthetic age spectra following the approach of Lovera et al. (1989), which are compared to the measured age spectra. The program then implements a controlled random search algorithm (Price, 1997) to converge on a set of best-fit thermal histories. Additional details on the *Arvert* modeling program are provided by Harrison et al. (2005) and the software is accessible at this link: <https://eesarchive.lehigh.edu/EESdocs/geochron/software.html>

Modeling was done iteratively to explore the impact of various parameters of the modeling, with the models presented providing the best fit to the data. Step heating experiments with obvious $^{40}\text{Ar}_\text{E}$ (see discussion by Lovera et al., 2002) were not included in the modeling process. Affected steps generally occurred at low temperatures, which is common and has been attributed to the release of metamorphic fluids from the decrepitation of fluid inclusions (Harrison et al., 1993). In general, we included steps in the modeling when the subsequent step heating experiment, whether an isothermal or higher-T step, yielded a similar or older age, consistent with volume diffusion. Cooling histories were limited to monotonic cooling only (no reheating permitted) as there is little geologic evidence of significant heat sources following the Cretaceous emplacement of the Tea Cup pluton and reheating allows for non-unique thermal histories. There are some Oligocene basaltic dikes present in parts of the Tea Cup pluton (Wong et al., 2015) but they are typically only 0.3-1.0 meters thick and are relatively minor volumetrically, so they likely had a minimal and highly transitory impact on the thermal history of the block. Care was also taken to avoid sampling nearby any dike exposure, further minimizing any potential thermal impact on the samples.

TABLE S1. K-FELDSPAR SAMPLE LOCATIONS FROM THE GRAYBACK FAULT BLOCK

Sample name	UTM Easting (m)¹	UTM Northing (m)	Paleodepth (km)²	Sample lithology	Notes
GR-19	497166	3654489	3.6	Proterozoic Ruin Granite	Megacrystic texture
GR-1	493862	3656744	5.9	Cretaceous Tea Cup pluton	Near inferred roof of pluton
GR-2	489985	3658850	10.1	Cretaceous Tea Cup pluton	
GR-27	488693	3660021	11.4	Pegmatite dike within Tea Cup pluton	
GR-8	488179	3660707	12.4	Cretaceous Tea Cup pluton	Deepest paleodepth exposed within the block

¹ All UTM coordinates are reported in the NAD27 CONUS datum.

² Paleodepth calculations follow the approach of Howard and Foster (1996)

REFERENCES CITED

- Duffield, W. A., and Dalrymple, G. B., 1990, The Taylor Creek Rhyolite of New Mexico: a rapidly emplaced field of lava domes and flows: *Bulletin of Volcanology*, 52, 475-487.
- Renne, P. R., Swisher, C. C., Deino, A. L., Karner, D. B., Owens, T. L., and DePaolo, D. J., 1998, Intercalibration of standards, absolute ages and uncertainties in ⁴⁰Ar/³⁹Ar dating: *Chemical Geology*, 145(1-2), 117-152.
- Lovera, O. M., 1992, Computer programs to model ⁴⁰Ar/³⁹Ar diffusion data from multidomain samples: *Computers & Geosciences*, 18(7), 789-813.
- Lovera, O. M., Grove, M., Harrison, T. M., and Mahon, K. I., 1997, Systematic analysis of K-feldspar ⁴⁰Ar/³⁹Ar step heating results: I. Significance of activation energy determinations: *Geochimica et Cosmochimica Acta*, 61(15), 3171-3192.
- Harrison, T. M., Grove, M., Lovera, O. M., and Zeitler, P. K., 2005, Continuous thermal histories from inversion of closure profiles: *Reviews in Mineralogy and Geochemistry*, 58(1), 389-409.

- Lovera, O. M., Richter, F. M., & Harrison, T. M., 1989, The $^{40}\text{Ar}/^{39}\text{Ar}$ thermochronometry for slowly cooled samples having a distribution of diffusion domain sizes: *Journal of Geophysical Research: Solid Earth*, 94(B12), 17917-17935.
- Lovera, O. M., Grove, M., and Harrison, T. M., 2002, Systematic analysis of K-feldspar $^{40}\text{Ar}/^{39}\text{Ar}$ step heating results II: Relevance of laboratory argon diffusion properties to nature: *Geochimica et Cosmochimica Acta*, 66(7), 1237-1255.
- Harrison, T. M., Heizler, M. T., and Lovera, O. M., 1993, In vacuo crushing experiments and K-feldspar thermochronometry: *Earth and Planetary Science Letters*, 117(1-2), 169-180.
- Wong, M. S., Gleason, D. M., O'Brien, H. P., and Idleman, B. D., 2015, Confirmation of a low pre-extensional geothermal gradient in the Grayback normal fault block, Arizona: Structural and AHe thermochronologic evidence: *Geological Society of America Bulletin*, 127(1-2), 200-210.

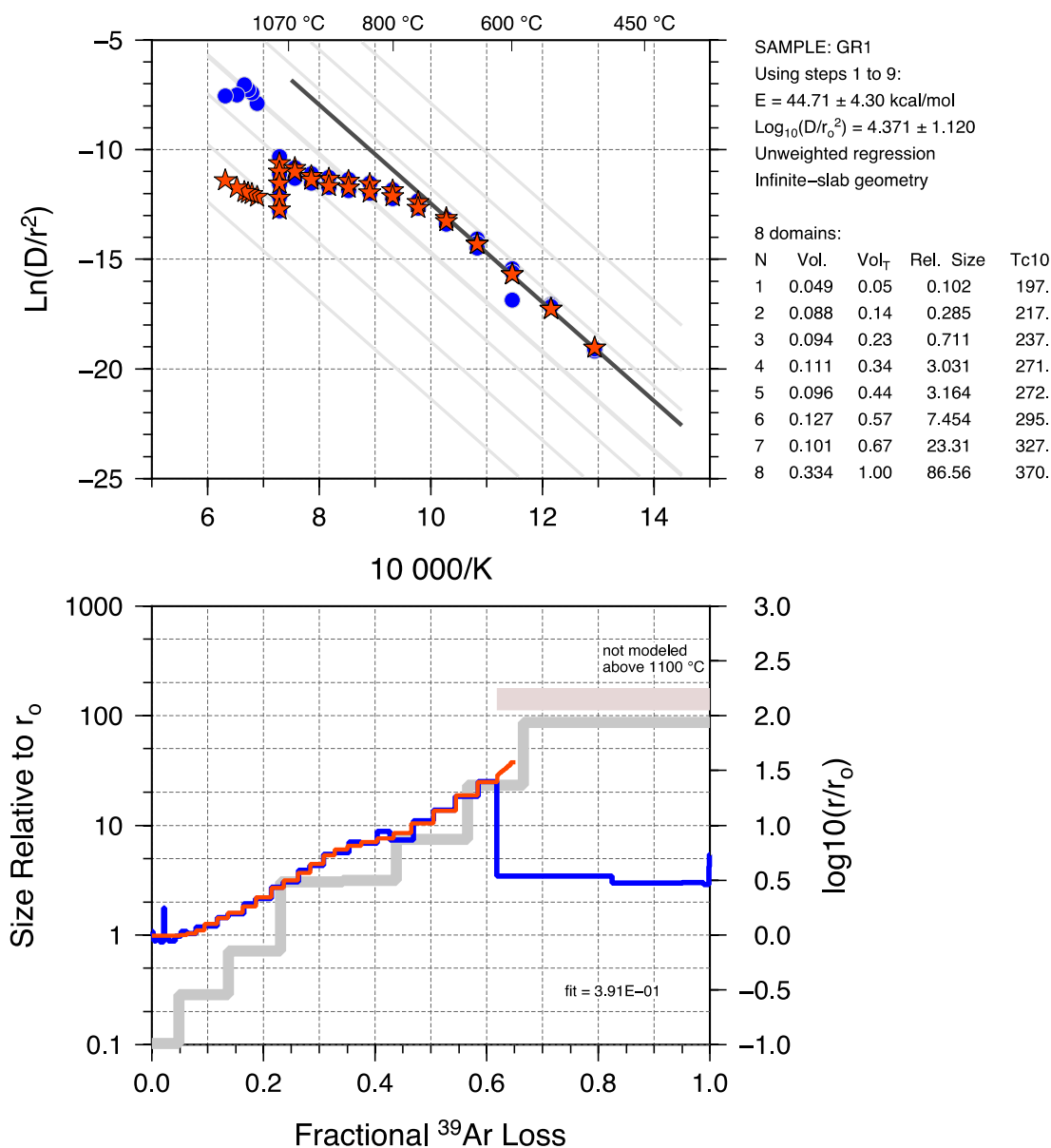


Figure S1. Top - Arrhenius plot of sample GR-1 showing measured diffusivities (blue circles), modelled diffusivities (red stars), and the reference Arrhenius law (black line) determined from the low-temperature steps. Bottom – Log(r/r_0) spectrum (right axis) showing measured (blue) and modeled (red) data. Gray line shows the relative size and volume fraction of the modeled diffusion domains (left axis).

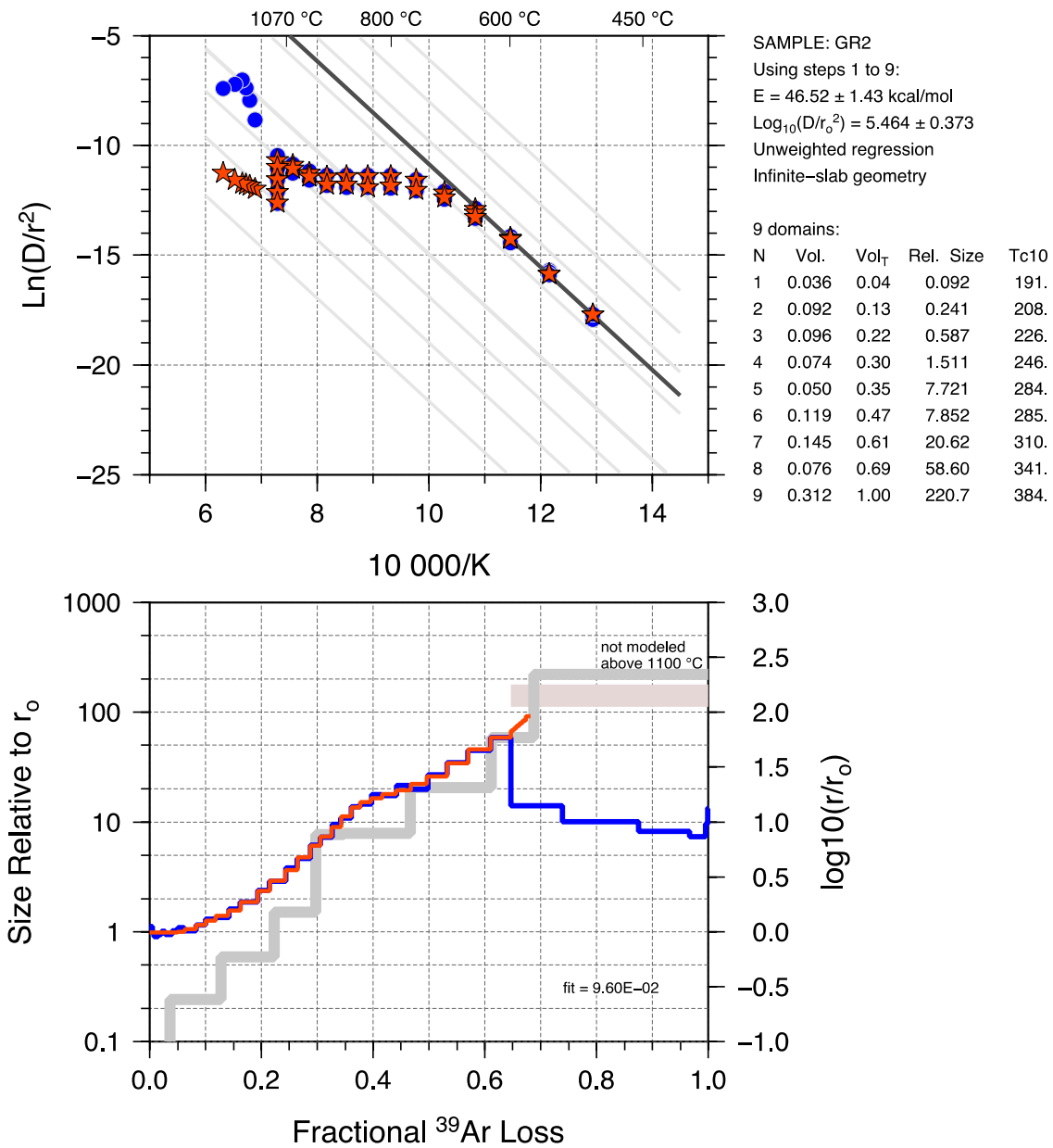


Figure S2. Top - Arrhenius plot of sample GR-2 showing measured diffusivities (blue circles), modelled diffusivities (red stars), and the reference Arrhenius law (black line) determined from the low-temperature steps. Bottom - Log(r/r_0) spectrum (right axis) showing measured (blue) and modeled (red) data. Gray line shows the relative size and volume fraction of the modeled diffusion domains (left axis).

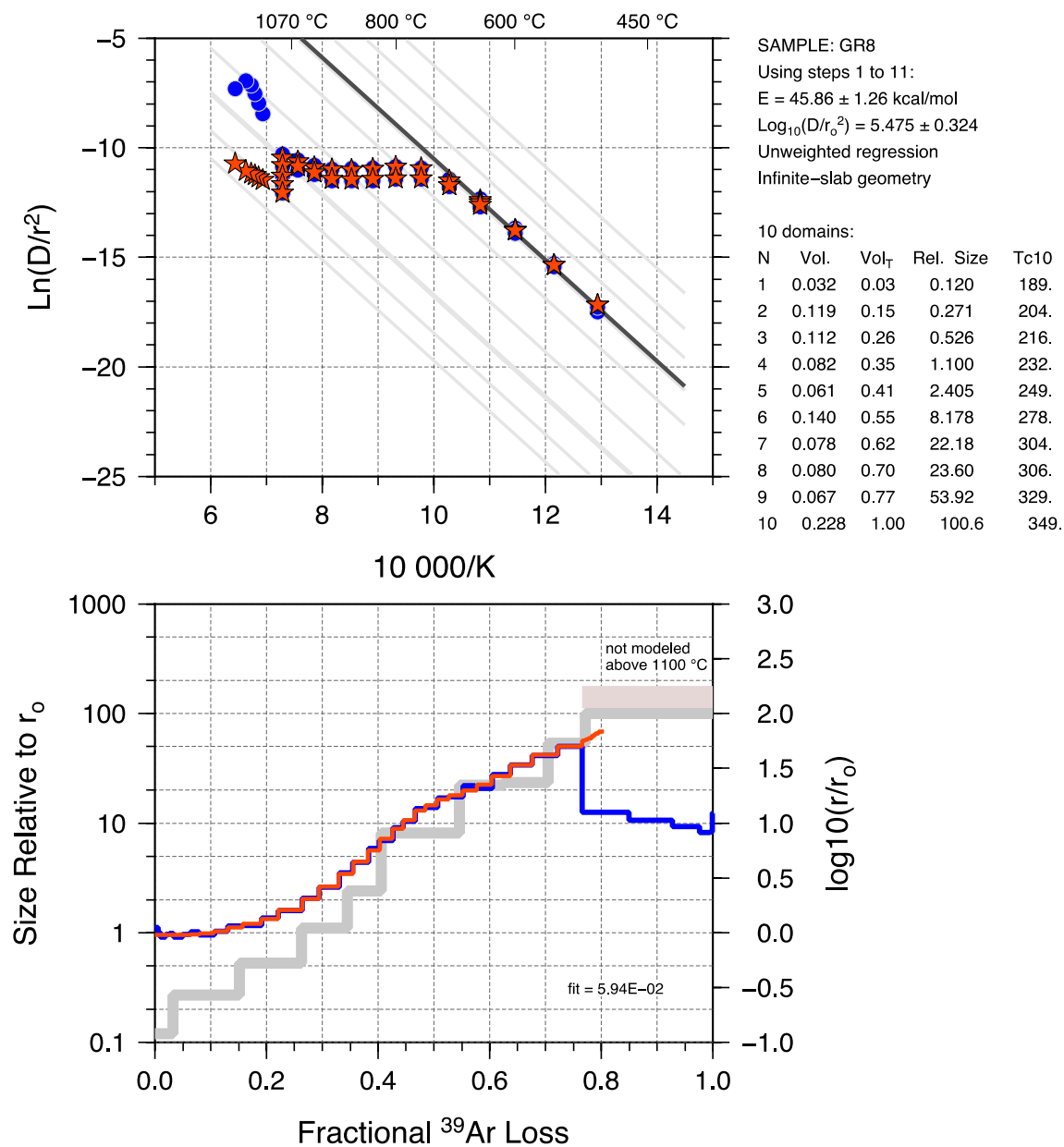


Figure S3. Top - Arrhenius plot of sample GR-8 showing measured diffusivities (blue circles), modelled diffusivities (red stars), and the reference Arrhenius law (black line) determined from the low-temperature steps. Bottom – Log(r/r_0) spectrum (right axis) showing measured (blue) and modeled (red) data. Gray line shows the relative size and volume fraction of the modeled diffusion domains (left axis).

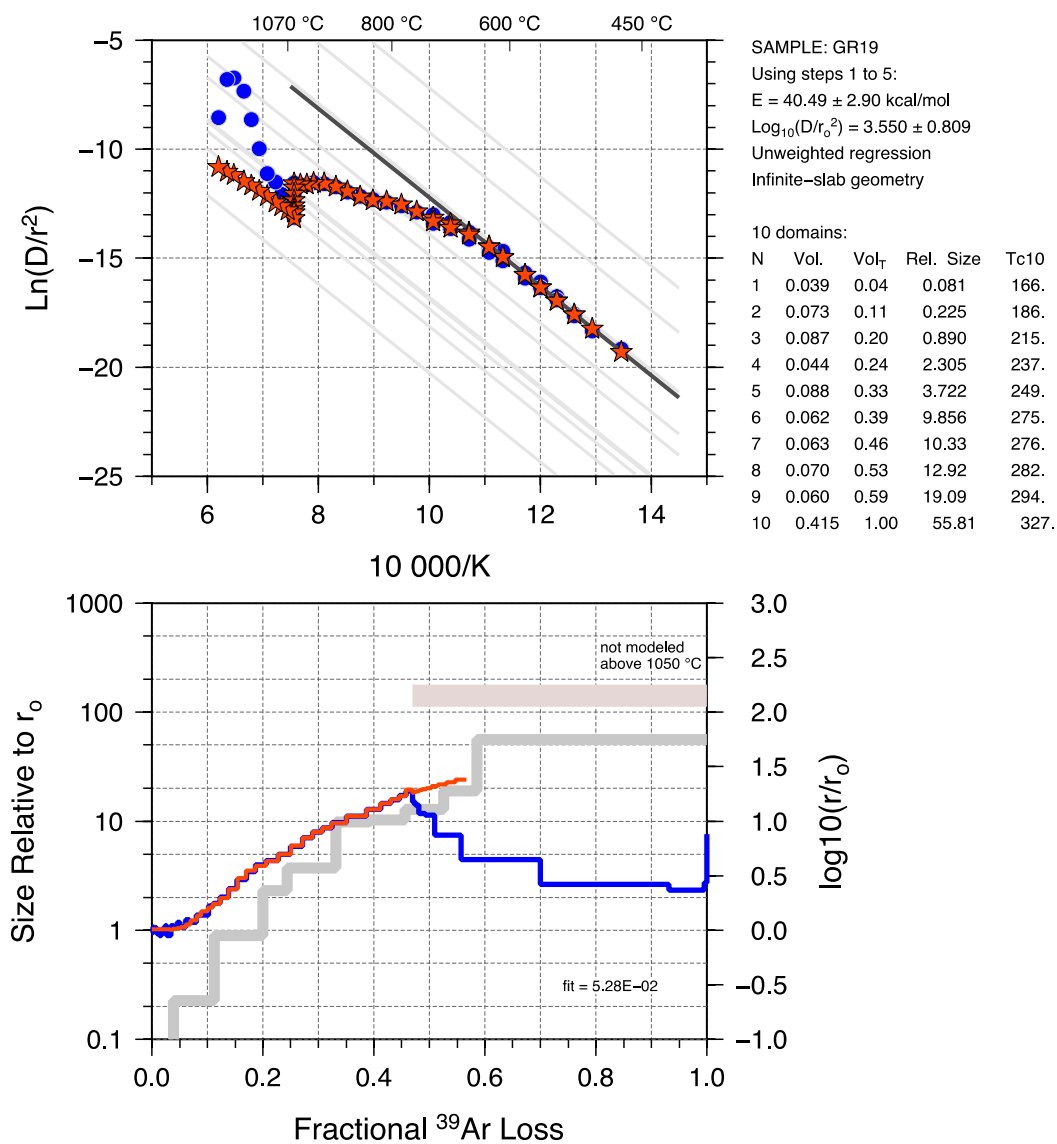


Figure S4. Top - Arrhenius plot of sample GR-19 showing measured diffusivities (blue circles), modelled diffusivities (red stars), and the reference Arrhenius law (black line) determined from the low-temperature steps. Bottom – Log(r/r_0) spectrum (right axis) showing measured (blue) and modeled (red) data. Gray line shows the relative size and volume fraction of the modeled diffusion domains (left axis).

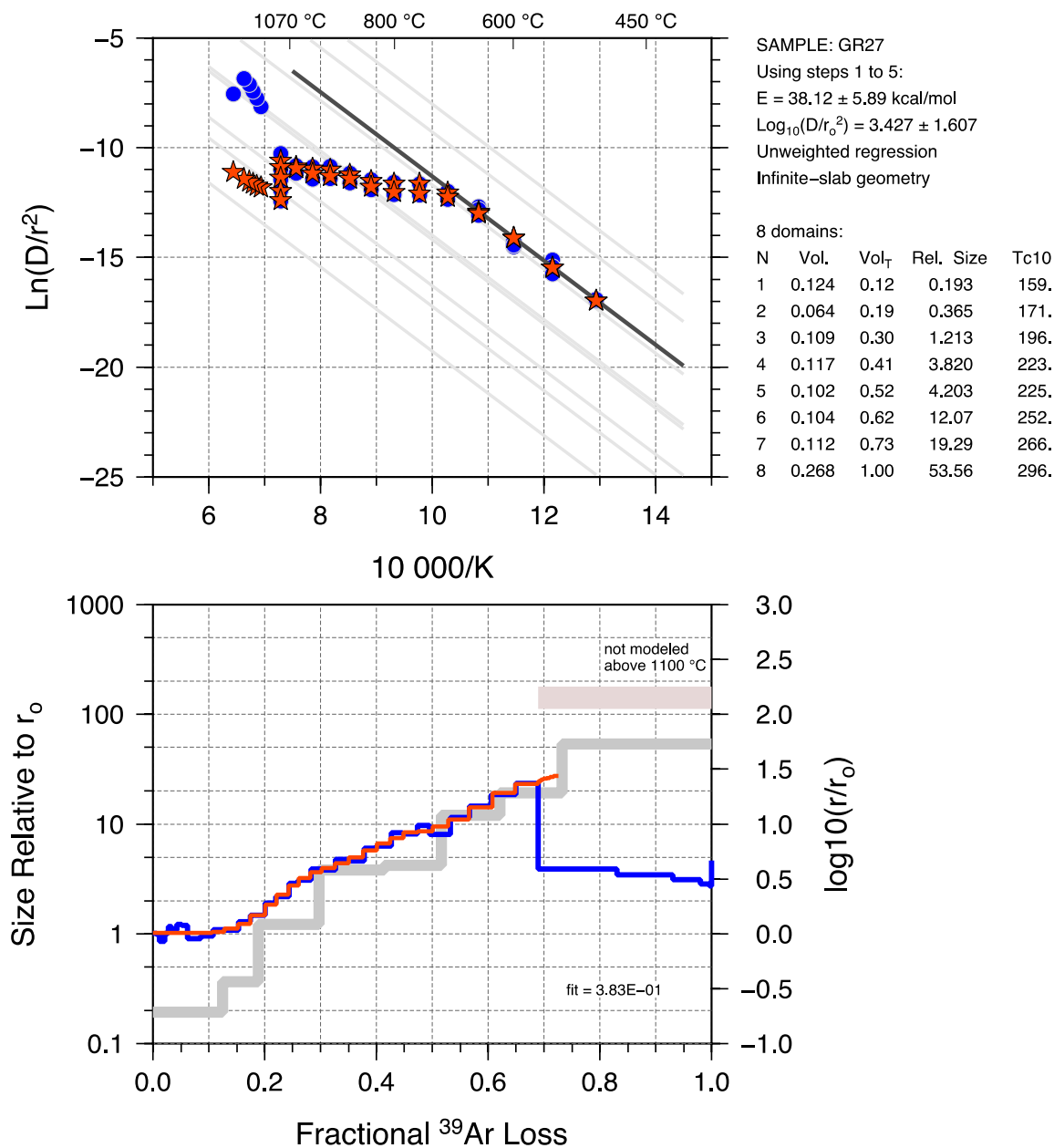


Figure S5. Top - Arrhenius plot of sample GR-27 showing measured diffusivities (blue circles), modelled diffusivities (red stars), and the reference Arrhenius law (black line) determined from the low-temperature steps. Bottom - $\text{Log}(r/r_0)$ spectrum (right axis) showing measured (blue) and modeled (red) data. Gray line shows the relative size and volume fraction of the modeled diffusion domains (left axis).

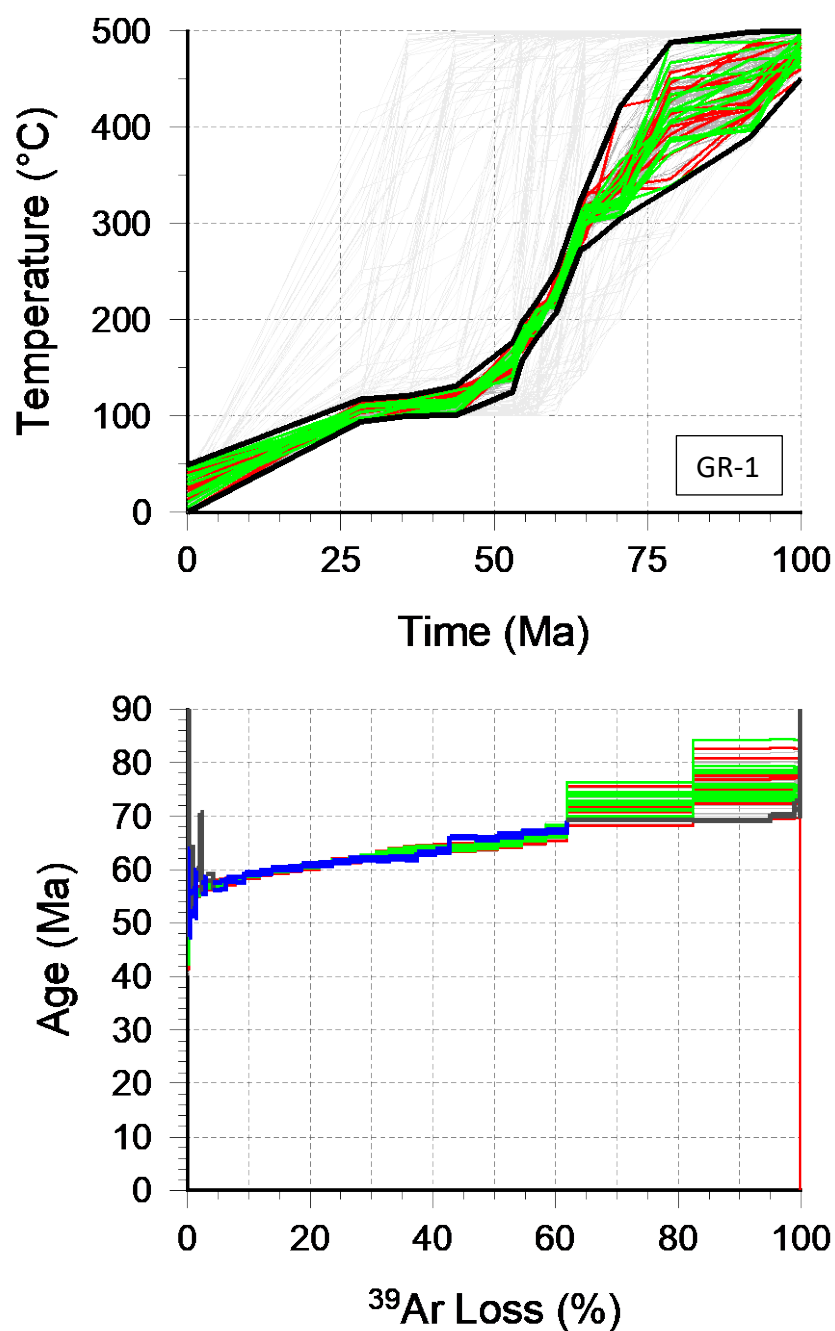


Figure S6. Top – Thermal histories based on MDD modeling of sample GR-1, showing the best-fit 15 thermal models out of the final pool (green), the worst-fit 15 out of the final pool (red), and the remaining models (gray). Also shown are the upper and lower bounds of all the models (black lines) and the initial Monte Carlo histories (faint gray). Bottom – The measured age spectrum (blue) compared with the synthetic age spectra (green and red, corresponding to the best 15 and worst 15 models of the final pool) generated by the MDD thermal models. Step heating experiments that were omitted from the modeling are shown in dark gray.

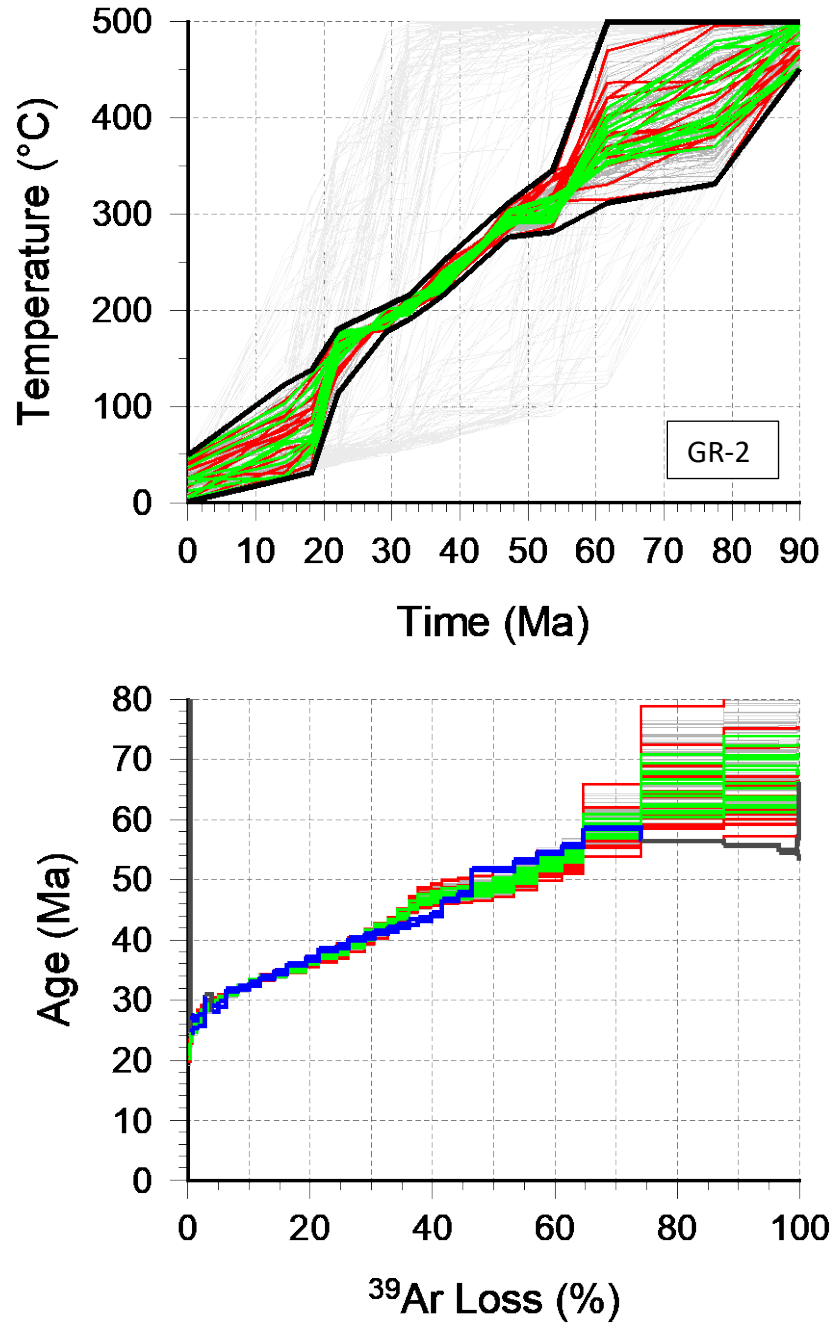


Figure S7. Top – Thermal histories based on MDD modeling of sample GR-2, showing the best-fit 15 thermal models out of the final pool (green), the worst-fit 15 out of the final pool (red), and the remaining models (gray). Also shown are the upper and lower bounds of all the models (black lines) and the initial Monte Carlo histories (faint gray). Bottom – The measured age spectrum (blue) compared with the synthetic age spectra (green and red, corresponding to the best 15 and worst 15 models of the final pool) generated by the MDD thermal models. Step heating experiments that were omitted from the modeling are show in dark gray.

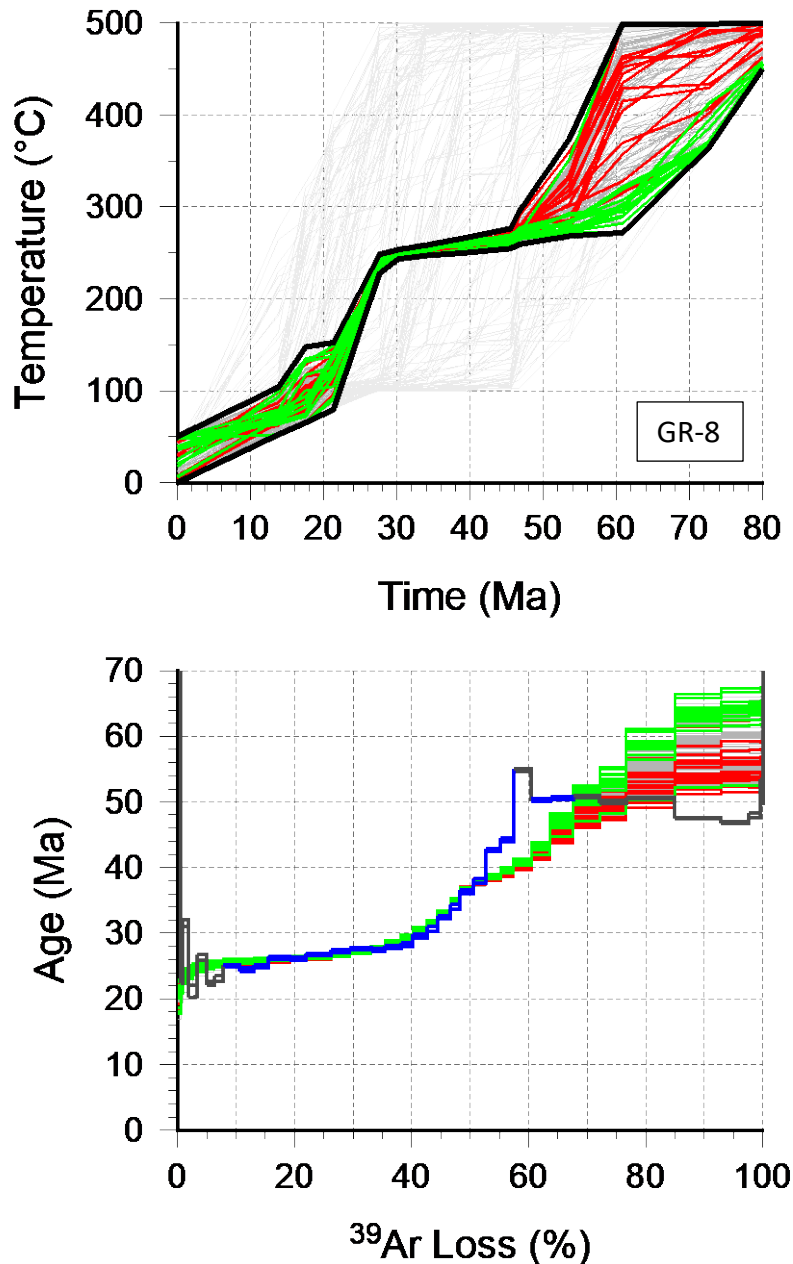


Figure S8. Top – Thermal histories based on MDD modeling of sample GR-8, showing the best-fit 15 thermal models out of the final pool (green), the worst-fit 15 out of the final pool (red), and the remaining models (gray). Also shown are the upper and lower bounds of all the models (black lines) and the initial Monte Carlo histories (faint gray). Bottom – The measured age spectrum (blue) compared with the synthetic age spectra (green and red, corresponding to the best 15 and worst 15 models of the final pool) generated by the MDD thermal models. Step heating experiments that were omitted from the modeling are shown in dark gray. The steps in the first ~8% of gas release were omitted from modeling due to the presence of excess Ar as indicated by older ages. The mismatch between the synthetic and measured spectra from 50-65% gas release is likely due to the presence of modest excess Ar that is suggested by slightly older ages that drop back down to younger ages at higher-T steps. Steps above 1100 °C (>70% gas release) are likely past the K-feldspar melting point and were not included in the modeling.

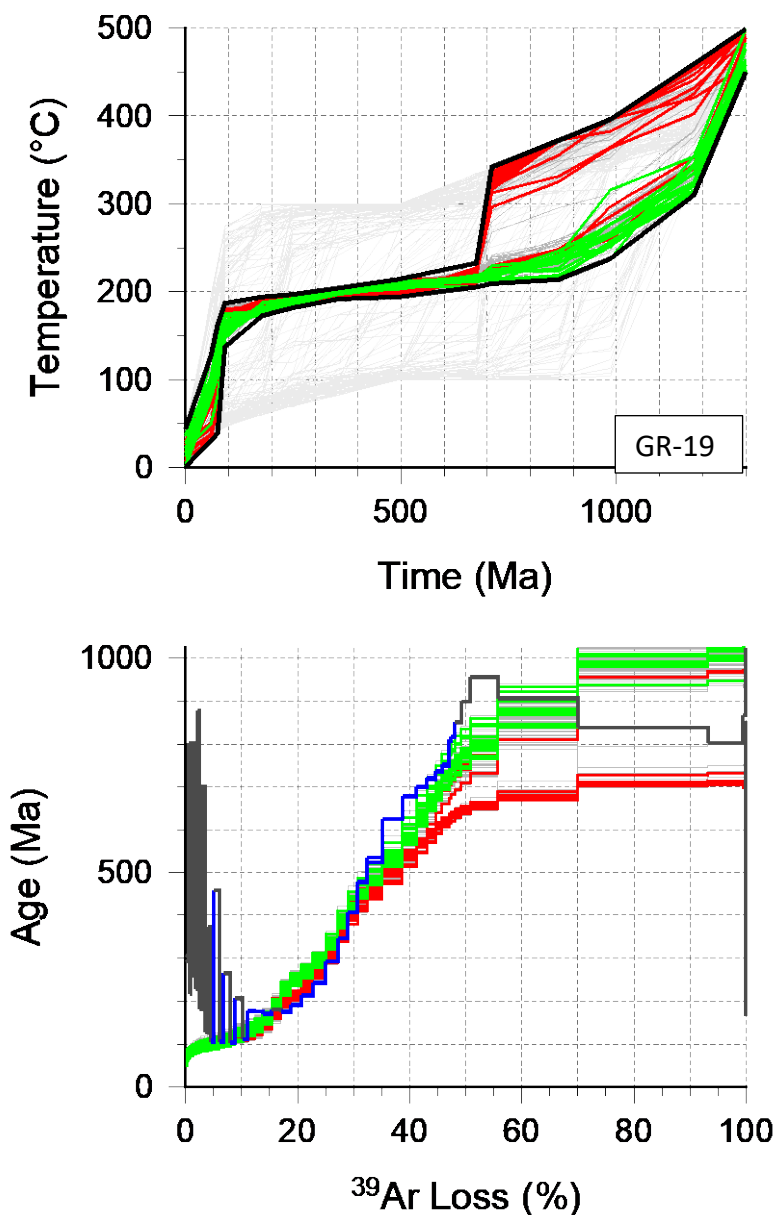


Figure S9. Top – Thermal histories based on MDD modeling of sample GR-19, showing the best-fit 15 thermal models out of the final pool (green), the worst-fit 15 out of the final pool (red), and the remaining models (gray). Also shown are the upper and lower bounds of all the models (black lines) and the initial Monte Carlo histories (faint gray). Bottom – The measured age spectrum (blue) compared with the synthetic age spectra (green and red, corresponding to the best 15 and worst 15 models of the final pool) generated by the MDD thermal models. Step heating experiments that were omitted from the modeling are shown in dark gray. Low-T steps in the first 10% of gas release were omitted from the modeling due to the presence of extensive excess Ar as indicated by much older ages. Some duplicate or triplicate steps were included at low-T if the subsequent step age was the same age or older, consistent with volume diffusion. Steps above ~50% gas release were not included in the modeling because they are above 1100 °C, which is likely above the K-feldspar melting temperature and not governed by volume diffusion.

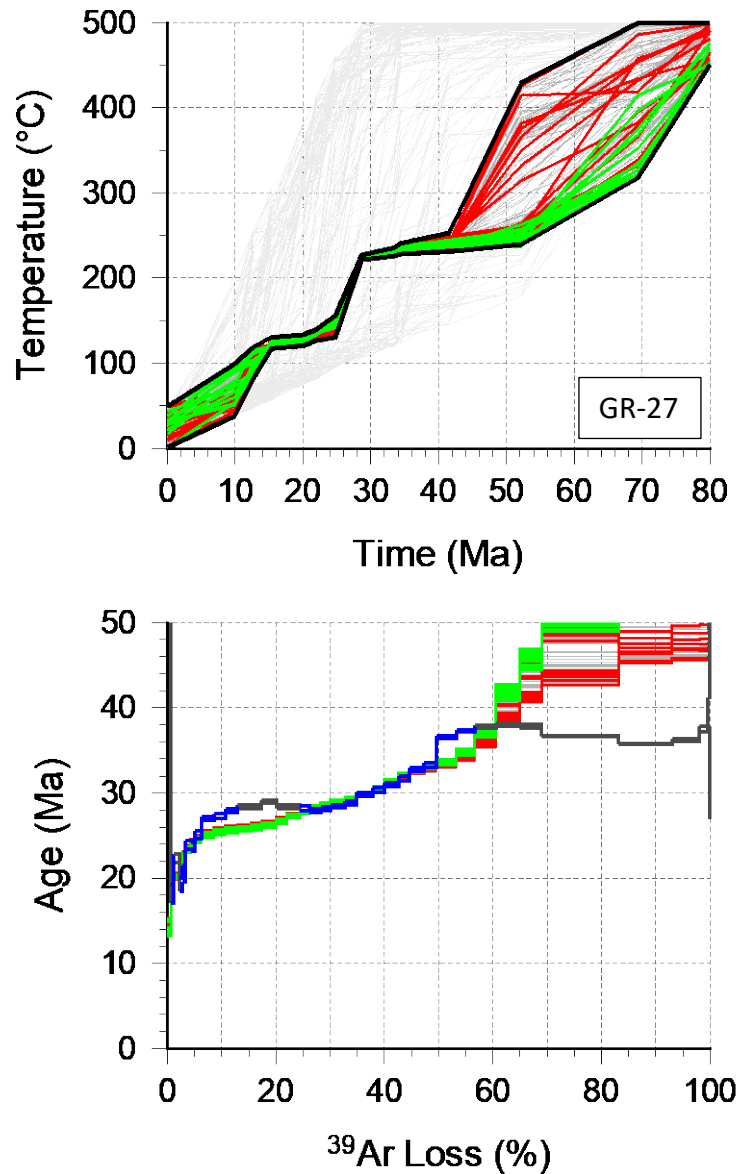


Figure S10. Top – Thermal histories based on MDD modeling of sample GR-27, showing the best-fit 15 thermal models out of the final pool (green), the worst-fit 15 out of the final pool (red), and the remaining models (gray). Also shown are the upper and lower bounds of all the models (black lines) and the initial Monte Carlo histories (faint gray). Bottom – The measured age spectrum (blue) compared with the synthetic age spectra (green and red, corresponding to the best 15 and worst 15 models of the final pool) generated by the MDD thermal models. Step heating experiments that were omitted from the modeling are shown in dark gray. Low-T steps from ~15-25% gas release were not included in the modeling due to the likely presence of modest amounts of excess Ar as evident from the slight fall in ages from 25-35% gas release. Steps above ~60% gas release were not included in the modeling because they are above 1100 °C, which is likely above the K-feldspar melting temperature and not governed by volume diffusion. This results in the mismatch between the synthetic and measured spectra at high-T steps.